DOI: 10.1002/anie.200901375

Single-Molecule Studies

Determination of the Superradiance Coherence Length of Directly Linked Linear Porphyrin Arrays at the Single-Molecule Level**

Jaesung Yang, Hyejin Yoo, Naoki Aratani, Atsuhiro Osuka, and Dongho Kim**

The ever-growing demand for device miniaturization has driven researchers in molecular photonics to pay considerable attention to the development of single-molecule photonic devices.[1–13] One fascinating approach is to utilize strongly coupled multichromophoric systems, because the excitonic interactions among the chromophores underlie extremely rapid and efficient excitation energy transfer, as observed in photosynthetic light-harvesting (LH) complexes by ultrafast spectroscopic techniques.[14–16] However, except for examination of the delocalized excited state of the B850 ring of an individual LH2 complex at cryogenic temperature,[17] the detailed mechanism of excitation energy transfer in strongly coupled molecular assemblies has scarcely been investigated at a single-molecule level. Nevertheless, it is crucial to understand this process in order to develop solid-state photonic devices approaching the ultimate limit of downsizing.

Herein, we present the use of single-molecule fluorescence spectroscopy (SMFS) to evaluate the exciton delocalization length observed by superradiance of a series of meso–meso directly linked zinc(II) porphyrin arrays (**Z***n* + **1**; $n = 0$–5; Figure 1a),[18] whose simple rodlike structures and ample electronic interactions make them suitable for application as molecular photonic wires. Furthermore, we describe how the excited-state behaviors of the arrays change according to the photobleaching sequence of individual chromophores. SMFS of the porphyrin arrays allows for appraisal of their functionalities in the solid state and provides insight into the construction of realistic photonic wires that can efficiently transport excitation energy over a long distance.

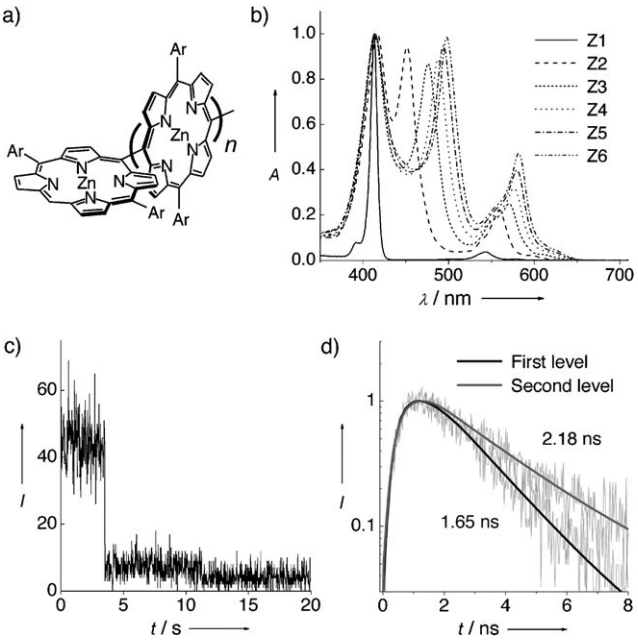

Figure 1. a) Molecular structures of meso–meso directly linked zinc(II) porphyrin arrays (**Z***n* + **1**; $n = 0$–5). Ar = 3,5-$(OC_8H_{17})_2C_6H_3$. b) UV/Vis steady-state absorption spectra of the porphyrin arrays normalized at approximately 413 nm. c) A typical fluorescence intensity trajectory (FIT) of a single **Z2** molecule. *I* represents the number of counts per 20 ms. d) Fluorescence decay profiles corresponding to each emissive level of the FIT shown in (c). Details of the decay analysis are given in Table S2 in the Supporting Information. The superradiance coherence size (L_s) of the molecule was calculated to be 1.8.

The absorption spectra of the porphyrin arrays exhibit split Soret bands as a result of exciton coupling (Figure 1b and Figure S1 in the Supporting Information). Given the excitation wavelength of 470 nm in the region of the low-energy Soret band, this feature provides an interesting characteristic of the fluorescence intensity trajectories (FITs) of the arrays, that is, the fluorescence intensity of a single molecule as a function of time. Figure 1c displays a typical FIT of a single **Z2** molecule in which the fluorescence intensity of the second emissive level shows an order of magnitude drop from the first level, with a concurrent increase in the fluorescence lifetime from 1.65 to 2.18 ns (Figure 1d). These changes are ascribed to the breakdown of exciton coupling upon photobleaching of one chromophore, because the remaining porphyrin monomer has only a negligible oscillator strength at the excitation wavelength of 470 nm.

For longer porphyrin arrays, in the case when the FITs show the same number of steps as porphyrin units, the

[*] Dr. N. Aratani, Prof. Dr. A. Osuka
Department of Chemistry, Graduate School of Science
Kyoto University, Sakyo-ku, Kyoto 606-8502 (Japan)
E-mail: osuka@kuchem.kyoto-u.ac.jp
J. Yang, H. Yoo, Prof. Dr. D. Kim
Department of Chemistry and Spectroscopy Laboratory for Functional π-Electronic Systems, Yonsei University
262 Seongsanno, Seodaemun-gu, Seoul 120-749 (Korea)
Fax: (+82) 2-2123-2434
E-mail: dongho@yonsei.ac.kr

[**] This research was financially supported by the Star Faculty and World Class University (No. 2008-8-1955) Programs of the Ministry of Education, Science, and Technology (MEST) of Korea (D.K.). J.Y. and H.Y. acknowledge the fellowship of the BK21 program from MEST. The work at Kyoto University was supported by a Grant-in-Aid (A) for Scientific Research (No. 19205006) from the Ministry of Education, Culture, Sports, Science, and Technology of Japan (A.O.).

Supporting information for this article is available on the WWW under http://dx.doi.org/10.1002/anie.200901375.

simultaneous analysis of the FITs and fluorescence lifetimes allows for observation of the photobleaching dynamics based on the photobleaching sequence of individual chromophores. Remnant FITs showing fewer steps than the number of porphyrin units, which may arise from the generation of a fluorescence trapping site that quenches excitations along the entire array,[19] were excluded because they were not suitable for the purpose of the analysis.

As shown in Figure 2, the photobleaching dynamics of **Z3** can be classified into two representative cases. In both FITs, the fluorescence lifetimes of the first emissive levels are shorter than those in **Z2**, which is clearly indicative of enhanced exciton delocalization. However, a striking difference is observed at the second emissive level. In Figure 2a, the second emissive level in the FIT shows 11 times higher fluorescence intensity than that of the third level, and the fluorescence lifetime of 1.64 ns is intermediate between those of the first (1.59 ns) and third (2.07 ns) levels. Because this feature is similar to that found for **Z2**, we attribute it to the photobleaching of one of a terminal porphyrin unit (Figure 2a, schematic). On the other hand, when the central porphyrin unit is photobleached first (Figure 2b, schematic), the remaining two chromophores are separated from each other by approximately 17 Å, and the coupling strength diminishes by an order of magnitude. In this case, as shown in

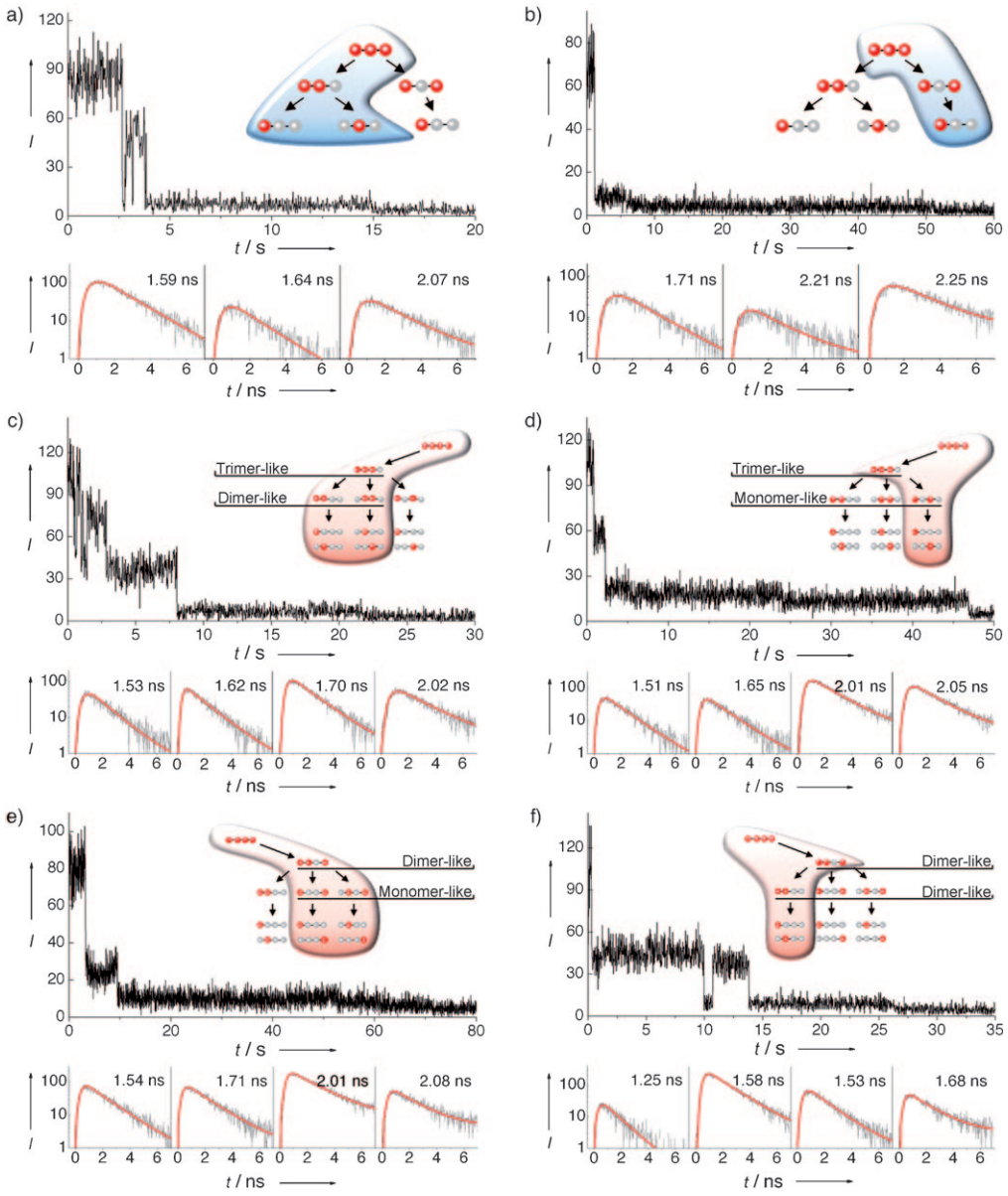

Figure 2. Representative FITs (*I* represents the number of counts per 20 ms) and fluorescence decay profiles corresponding to each emissive level (details of the decay analysis are given in Table S2 in the Supporting Information) of **Z3** molecules exhibiting a) dimer-like and b) monomer-like behavior at the second emissive level in the FITs, and of **Z4** molecules exhibiting c) trimer- and dimer-like, d) trimer- and monomer-like, e) dimer- and monomer-like, and f) dimer- and dimer-like behavior at the second and third emissive levels in the FITs. The schematic representations in each part display photobleaching sequences compatible with the experimental data. The L_s values for each molecule were calculated to be 2.7, 2.7, 3.6, 3.8, 3.7, and 3.7 (a–f, respectively).

Figure 2b, the second emissive level in the FIT carries only twice the intensity and a similar lifetime as the third level.

The photobleaching dynamics of **Z4** can be classified into four representative cases according to the characteristics of the second and third emissive levels in the FITs. Again, the first emissive levels show even shorter fluorescence lifetimes, from which we can infer the further augmentation of the exciton delocalization. For simplicity, we refer to the porphyrin units in **Z4** as p1–p4, starting from the left.

In Figure 2c, the fluorescence intensities of the second and third emissive levels are 12 and 7 times higher, respectively, than that of the fourth level, and the respective fluorescence lifetimes of 1.62 and 1.70 ns are well-matched with those observed for **Z2** and **Z3** (Table S1 in the Supporting Information). It is thought that the molecule exhibits trimer- and dimer-like behavior at the second and third levels, respectively, which can occur when the molecule follows photobleaching sequences p4→p3→p1 (or p2) or p4→p1→p2 (or p3; Figure 2c, schematic). On the other hand, the third emissive level of the FIT in Figure 2d shows monomer-like behavior with only twice the intensity and a similar lifetime as the fourth level. We attribute this feature to the photobleaching sequence p4→p2→p1 (or p3; Figure 2d, schematic). If one of the inner porphyrin units photobleaches first, the molecule shows dimer-like behavior at the second emissive level. In Figure 2e, the second emissive level of the FIT has only half the intensity of that in Figure 2d, with a slightly increased lifetime of 1.71 ns. Because the molecule exhibits dimer- and monomer-like behavior at the second and third levels, we assign this molecule the photobleaching sequences p3→p2→p1 (or p4) or p3→p1→p2 (or p4; Figure 2e, schematic). As the last case, the FIT in Figure 2f shows similar fluorescence intensities and lifetimes of 1.58 and 1.53 ns, respectively, at both the second and the third emissive levels, which can be thought to arise from dimer-like behavior. In this case, the molecule might follow the photobleaching sequence p3→p4→p1 (or p2) (Figure 2f, schematic).

Considering the above observations, we examined the superradiance effect in the porphyrin arrays to evaluate the extent of exciton delocalization. The superradiance can be quantified using the superradiance coherence size, which is defined as the ratio of the radiative decay rate of the array to that of a monomer ($L_s = k_{rad,array}/k_{rad,monomer}$),[15,16,20] because the radiative decay rate ($k_{rad} = \Phi_f/\tau_f$; Φ_f = fluorescence quantum yield, τ_f = fluorescence lifetime) of the array increases when the constituent chromophores interact with each other and radiate in phase. In our approach, the radiative decay rates for the array and the monomer were calculated using fluorescence lifetimes at the first and last emissive levels, respectively, in the FITs and fluorescence quantum yields from bulk measurements (Table S1 in the Supporting Information), as it is impossible to measure them at the single-molecule level. The agreement between the tendency of the photon count rates per porphyrin unit for the arrays and that of the fluorescence quantum yields in solution rationalizes this assumption (Figure S2 in the Supporting Information).

For the **Z2** molecule in Figure 1c, we obtained an L_s value of 1.8; for **Z3**, the L_s value was 2.7 for both of the molecules in Figure 2a,b. The **Z4** molecules in Figure 2c–f exhibit L_s values of 3.6, 3.8, 3.7, and 3.7. The obtained L_s values for each array are slightly smaller than the ideal values of 2, 3, and 4, which would be expected for full exciton delocalization. The site-energy variation of individual chromophores (static disorder) and the exciton–phonon coupling (dynamic disorder), as we observe the fluorescence of thermalized excitons, might account for this discrepancy. Even so, this result indicates that the superradiance coherence size increases linearly as the array becomes longer.

In the longer arrays, the superradiance coherence size seems to show saturation behavior. Figure 3 displays the representative FITs of single **Z5** and **Z6** molecules with five and six distinct intensity levels, respectively. Interestingly, the fluorescence lifetimes of the first emissive levels for both molecules reach a saturated value of about 1.5 ns (Figure 3a,b, insets). This finding suggests that the superradiance coherence size no longer increases linearly with the number of porphyrin units. L_s values of 4.4 and 5.0 were obtained for the **Z5** and **Z6** molecules in Figure 3.

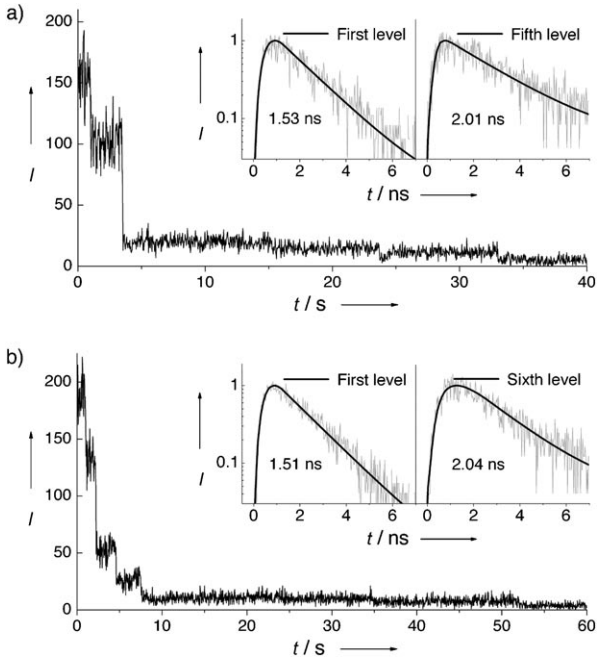

Figure 3. Representative FITs (*I* represents the number of counts per 20 ms) and fluorescence decay profiles corresponding to the first and last emissive levels (details of the decay analysis are given in Table S2 in the Supporting Information) a) of the **Z5** molecule ($L_s = 4.4$) and b) of the **Z6** molecule ($L_s = 5.0$).

We carried out a statistical analysis by collecting 64 single-molecule datasets for each array. The probability of acquiring FITs for the analysis gradually decreases as the array becomes longer owing to the increased likelihood of generating fluorescence trapping sites that quench excitation along the entire array (Figure 4a, red squares). In Figure 4b, a distribution of the superradiance coherence size shows a progressive shift upward to **Z4**, after which it becomes saturated at a value around 4.5, which is clarified in a plot of the averaged L_s

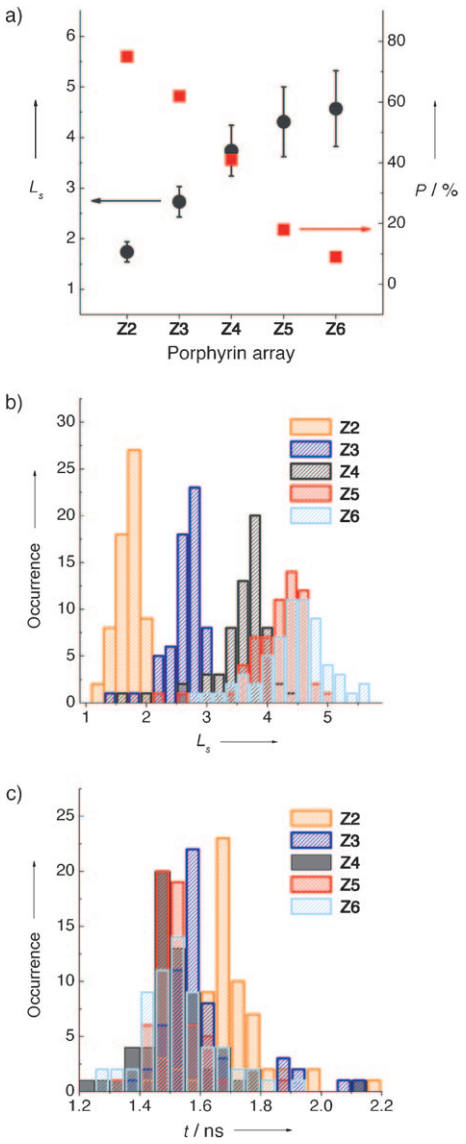

Figure 4. a) A plot of averaged L_s values with standard deviations (black circles) and the percentage of FITs showing the same number of steps as porphyrin units (red squares). b) Histograms for superradiance coherence sizes (L_s) of the arrays from **Z2** to **Z6**. c) Histograms for fluorescence lifetimes of the first emissive level in the FITs. Both histograms were constructed by collecting 64 single-molecule datasets for each array.

values (Figure 4a, black circles). Furthermore, the width of the distribution broadens with an increasing number of porphyrin units owing to various manifestations of the interplay between the excitonic coupling and the static and dynamic disorders in the longer arrays. The characteristics in the histogram of superradiance coherence size are corroborated by a trend in the fluorescence lifetimes at the first emissive level in the FITs, as shown in Figure 4c.

The superradiance coherence size depends on the exciton dynamics and geometry of molecular assemblies. However, when all dipoles in the assemblies are parallel, L_s provides a direct estimate of the exciton delocalization length.[15,16] Thus, for the investigated linear porphyrin arrays, four or five porphyrin units would be the best estimation of the exciton delocalization length at the single-molecule level, according to the histogram of superradiance coherence sizes (Figure 4b). This feature implies that four or five chromophores within the array behave as a coherently coupled exciton, whereas the light-signal transmission on a large scale resembles the hopping-like process of this exciton.

We should note that individual porphyrin arrays retain coherent excitonic interaction over several porphyrin units, even in the solid state at room temperature. Under the given experimental conditions, it is expected that the static and dynamic disorders greatly reduce the extent of exciton delocalization. Specifically, the static disorder might play an important role, because energy fluctuations between the chromophores become severe owing to the increase in the inhomogeneity of the surrounding medium. For the porphyrin arrays, the covalent direct linkage, with a short center-to-center distance of approximately 8.4 Å, facilitates the dipole interactions among the chromophores, and the orthogonal geometry imposed by a large steric hindrance allows for the linearity to be void of any energy sink. These properties probably minimize the disorders and thus contribute to the preservation of coherence and to the facile excitation energy transfer of the arrays in the solid state.

In summary, we have revealed that the excitonic interactions in directly linked porphyrin arrays are well conserved in the solid state at room temperature and that the interaction extends over four or five porphyrin units, which provides a perspective for the arrays to be utilized as a realistic solid-state photonic wire. Furthermore, our results allow for a better understanding of how the light-signal transmission occurs in these sorts of molecular assemblies at the single-molecule level and serve as a basis for the rational design of molecular wires for applications in molecular photonics.

Experimental Section

The synthesis of the porphyrin arrays is described elsewhere.[18] The spin-cast dilute film of the arrays embedded in poly(methyl methacrylate) was illuminated by a 470 nm picosecond-pulse diode laser with irradiation power of 200 W cm^{-2} at the sample. The fluorescence of single molecules was detected using a confocal microscope equipped with an avalanche photodiode. More details on sample preparation, experimental methods, and data analysis are provided in the Supporting Information.

Received: March 12, 2009
Published online: May 13, 2009

Keywords: energy transfer · exciton delocalization · fluorescence spectroscopy · porphyrinoids · single-molecule studies

[1] *Single Molecule Optical Detection, Imaging and Spectroscopy* (Eds.: T. Basché, W. E. Moerner, M. Orrit, U. P. Wild), Wiley-VCH, Weinheim, **1997**.
[2] B. Lounis, W. E. Moerner, *Nature* **2000**, *407*, 491–493.
[3] M. Irie, T. Fukaminato, T. Sasaki, N. Tamai, T. Kawai, *Nature* **2002**, *420*, 759–760.

[4] F. C. De Schryver, T. Vosch, M. Cotlet, M. Van der Auweraer, K. Müllen, J. Hofkens, *Acc. Chem. Res.* **2005**, *38*, 514 – 522.
[5] P. Tinnefeld, M. Sauer, *Angew. Chem.* **2005**, *117*, 2698 – 2728; *Angew. Chem. Int. Ed.* **2005**, *44*, 2642 – 2671.
[6] M. F. García-Parajó, J. Hernando, G. S. Mosteiro, J. P. Hoogenboom, E. M. H. P. van Dijk, N. F. van Hulst, *ChemPhysChem* **2005**, *6*, 819 – 827.
[7] a) M. Park, M.-C. Yoon, Z. S. Yoon, T. Hori, X. Peng, N. Aratani, J.-I. Hotta, H. Uji-i, M. Sliwa, J. Hofkens, A. Osuka, D. Kim, *J. Am. Chem. Soc.* **2007**, *129*, 3539 – 3544; b) J. Yang, M. Park, Z. S. Yoon, T. Hori, X. Peng, N. Aratani, P. Dedecker, J.-I. Hotta, H. Uji-i, M. Sliwa, J. Hofkens, A. Osuka, D. Kim, *J. Am. Chem. Soc.* **2008**, *130*, 1879 – 1884.
[8] H. Jin, D. A. Heller, J.-H. Kim, M. S. Strano, *Nano Lett.* **2008**, *8*, 4299 – 4304.
[9] a) R. W. Wagner, J. S. Lindsey, *J. Am. Chem. Soc.* **1994**, *116*, 9759 – 9760; b) D. Holten, D. F. Bocian, J. S. Lindsey, *Acc. Chem. Res.* **2002**, *35*, 57 – 69.
[10] H. L. Anderson, *Inorg. Chem.* **1994**, *33*, 972 – 981.
[11] M. P. Debreczeny, W. A. Svec, M. R. Wasielewski, *Science* **1996**, *274*, 584 – 587.
[12] R. E. Martin, F. Diederich, *Angew. Chem.* **1999**, *111*, 1440 – 1469; *Angew. Chem. Int. Ed.* **1999**, *38*, 1350 – 1377.
[13] G. D. Scholes, K. P. Ghiggino, A. M. Oliver, M. N. Paddon-Row, *J. Am. Chem. Soc.* **1993**, *115*, 4345 – 4349.
[14] R. Jimenez, S. N. Dikshit, S. E. Bradforth, G. R. Fleming, *J. Phys. Chem.* **1996**, *100*, 6825 – 6834.
[15] T. Pullerits, M. Chachisvilis, V. Sundström, *J. Phys. Chem.* **1996**, *100*, 10787 – 10792.
[16] Y. Zhao, T. Meier, W. M. Zhang, V. Chernyak, S. Mukamel, *J. Phys. Chem. B* **1999**, *103*, 3954 – 3962.
[17] A. M. van Oijen, M. Ketelaars, J. Köhler, T. J. Aartsma, J. Schmidt, *Science* **1999**, *285*, 400 – 402.
[18] N. Aratani, A. Osuka, Y. H. Kim, D. H. Jeong, D. Kim, *Angew. Chem.* **2000**, *112*, 1517 – 1521; *Angew. Chem. Int. Ed.* **2000**, *39*, 1458 – 1462.
[19] D. A. Vanden Bout, W.-T. Yip, D. Hu, D.-K. Fu, T. M. Swager, P. F. Barbara, *Science* **1997**, *277*, 1074 – 1077.
[20] M. Lippitz, C. G. Hübner, Th. Christ, H. Eichner, P. Bordat, A. Herrmann, K. Müllen, Th. Basché, *Phys. Rev. Lett.* **2004**, *92*, 103001.

